



UNIVERSITY OF LEEDS

This is a repository copy of *Graphene Oxide/Poly (N-isopropylacrylamide) Hybrid Film-based Near-infrared Light-driven Bilayer Actuators with Shape Memory Effect*.

White Rose Research Online URL for this paper:  
<http://eprints.whiterose.ac.uk/121547/>

Version: Accepted Version

---

**Article:**

Chen, Z, Cao, R, Ye, S et al. (3 more authors) (2018) Graphene Oxide/Poly (N-isopropylacrylamide) Hybrid Film-based Near-infrared Light-driven Bilayer Actuators with Shape Memory Effect. *Sensors and Actuators B: Chemical*, 255 (3). pp. 2971-2978. ISSN 0925-4005

<https://doi.org/10.1016/j.snb.2017.09.119>

---

© 2017 Elsevier B.V. This manuscript version is made available under the CC-BY-NC-ND 4.0 license <http://creativecommons.org/licenses/by-nc-nd/4.0/>

**Reuse**

This article is distributed under the terms of the Creative Commons Attribution-NonCommercial-NoDerivs (CC BY-NC-ND) licence. This licence only allows you to download this work and share it with others as long as you credit the authors, but you can't change the article in any way or use it commercially. More information and the full terms of the licence here: <https://creativecommons.org/licenses/>

**Takedown**

If you consider content in White Rose Research Online to be in breach of UK law, please notify us by emailing [eprints@whiterose.ac.uk](mailto:eprints@whiterose.ac.uk) including the URL of the record and the reason for the withdrawal request.



[eprints@whiterose.ac.uk](mailto:eprints@whiterose.ac.uk)  
<https://eprints.whiterose.ac.uk/>

## Accepted Manuscript

Title: Graphene Oxide/Poly (N-isopropylacrylamide) Hybrid Film-based Near-infrared Light-driven Bilayer Actuators with Shape Memory Effect

Authors: Ze Chen, Rui Cao, Sunjie Ye, Yuanhang Ge, Yingfeng Tu, Xiaoming Yang



PII: S0925-4005(17)31785-9  
DOI: <http://dx.doi.org/10.1016/j.snb.2017.09.119>  
Reference: SNB 23210

To appear in: *Sensors and Actuators B*

Received date: 27-4-2017  
Revised date: 17-7-2017  
Accepted date: 19-9-2017

Please cite this article as: Ze Chen, Rui Cao, Sunjie Ye, Yuanhang Ge, Yingfeng Tu, Xiaoming Yang, Graphene Oxide/Poly (N-isopropylacrylamide) Hybrid Film-based Near-infrared Light-driven Bilayer Actuators with Shape Memory Effect, *Sensors and Actuators B: Chemical* <http://dx.doi.org/10.1016/j.snb.2017.09.119>

This is a PDF file of an unedited manuscript that has been accepted for publication. As a service to our customers we are providing this early version of the manuscript. The manuscript will undergo copyediting, typesetting, and review of the resulting proof before it is published in its final form. Please note that during the production process errors may be discovered which could affect the content, and all legal disclaimers that apply to the journal pertain.

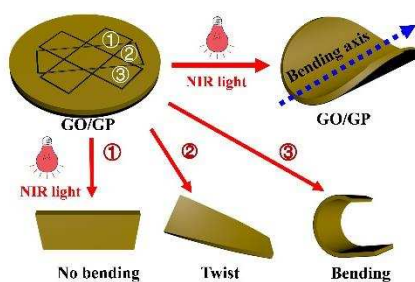
# Graphene Oxide/Poly (N-isopropylacrylamide) Hybrid Film-based Near-infrared Light-driven Bilayer Actuators with Shape Memory Effect

Ze Chen,<sup>1</sup> Rui Cao,<sup>1</sup> Sunjie Ye,<sup>2</sup> Yuanhang Ge,<sup>1</sup> Yingfeng Tu,<sup>1</sup> and Xiaoming Yang\*<sup>1</sup>

<sup>1</sup>State and Local Joint Engineering Laboratory for Novel Functional Polymeric Materials, Suzhou Key Laboratory of Macromolecular Design and Precision Synthesis, Jiangsu Key Laboratory of Advanced Functional Polymer Design and Application, Department of Polymer Science and Engineering, College of Chemistry, Chemical Engineering and Materials Science, Soochow University, Suzhou 215123, P. R. China.

<sup>2</sup>School of Physics and Astronomy, University of Leeds, Leeds, LS2 9JT, UK

\* Corresponding author. Tel.: +86-512-6588-4930; Fax: +86-512-6588-2130;



## Research highlights:

- A facile strategy two-step vacuum filtration has been developed to fabricate a NIR light-driven bilayer actuator.
- The actuator shows templated bending orientation exposed to NIR light, and exhibits shape memory effect.

- Complex deformation such as twist is realized due to the shape memory effect.

## ABSTRACT

Smart actuators with fast and reversible changes towards external stimuli have attractive potentials in diverse applications. Here, we present the rational design and facile fabrication of graphene oxide (GO) /poly (N-isopropylacrylamide) (PNIPAM) hybrid film-based bilayer actuators, which display efficient and reversible bending/unbending behaviors in response to repeated cycles of near-infrared (NIR) light irradiations. Our bilayer actuator comprises a layer of GO, and a layer of GO/PNIPAM (GP) hybrid, taking advantages of the NIR absorbance and photothermal conversion capability of GO, along with the thermo-responsiveness of PNIPAM. Upon NIR light irradiation, GO converts absorbed light into heat, which subsequently triggers the shrinkage of PNIPAM chains, leading to the bending of the bilayer actuator. Owing to the shape inertness of GO to the NIR light, repeated irradiations of NIR light cause the bilayer to shrink/relax in an asymmetric manner, consequently leading to reversible bending/unbending behaviors of the bilayer actuator. Remarkably, our actuator shows templated bending orientation once exposed to NIR light, and exhibits shape memory effect due to the incomplete recovery of PNIPAM chains. This shape memory effect is retained in rectangular strips cut from the original disk-shaped bilayer and is exploited to selectively achieve either bending or twisting deformation. As an interesting example

for potential practical utilization, a smart NIR light-driven forklift capable of lifting goods has been built by pinning one side of the bilayer film.

Keywords: Graphene oxide; PNIPAM; NIR actuator; Smart forklift truck

## 1. Introduction

Smart actuators offer a well controllable and reversible shape variations in response to environment stimuli, such as pH value, temperature., electricity, chemical energy, solvent, humidity, and light [1-9], and have great potential for developing innovative smart products, such as wearable computers, artificial muscles, electronic skins, smart microrobots, and so on [10,11]. Therefore, numerous research efforts have been dedicated to the rational design and construction of smart actuators on the basis of various material systems, including shape-memory alloy or polymers, stimuli-responsive materials, gels, liquid crystalline polymers and conjugated polymers [12-18].

With the purpose of developing novel smart actuators, lightweight and cost-effective carbon materials have been widely selected as preferred candidates owing to their enchanting advantages, such as mechanical robustness, chemical/physical stabilities, and high dimension variation properties [19]. In particular, as a new member in the carbon family, graphene and its derivatives s (e.g., graphene oxide, GO) have shown remarkable promise for fabricating smart actuators, because of their favorable physical/chemical properties (e.g., large surface area, extraordinary flexibility,

mechanical strength, conductivity, thermal conductivity, as well as excellent biocompatibility) [20-23]. To date, GO-based smart actuators have been engineered for both fundamental and applied research. Qu et al., successfully developed fiber-type smart actuators and robots via the laser reduction of GO fibers [24]. Sun et al. described a facile photoreduction strategy for constructing GO/reduced GO bilayer actuators utilizing focused sunlight irradiation [25]. These actuators employ water molecules as triggering molecules, i. e., when exposed to moisture, the GO layer swells as a result of the water-adsorption-induced expansion [26,27]. On the contrary, the reduced GO layer shows insignificant deformation, due to the fairly low level of water adsorption [14,28], resulting in asymmetric swelling, which accordingly induces reversible bending/unbending behaviors of the bilayer actuator. However, the motions of these actuators tend to be simple bending or straightening, more complicated performance such as twist is hardly realized.

On the other hand, photoresponsive materials offer programmable and reversible mechanical functionalities in photomechanical actuators, owing to their merits such as contactless actuation, local and remote control, omitted use of connecting wires or electrodes [29]. As a branch of photoresponsive materials, NIR-responsive nanocomposites have attracted numerous attentions thanks to their minimal invasion, and high transparency in the “biological window” [30]. They are usually composed of NIR-absorbing nanomaterials, e.g., anisotropic metal nanostructures, carbon nanotubes and graphene/GO, with a variety of soft matrices [31-35]. While GO exhibit optical

absorption in visible and NIR region, it shows a great photothermal conversion efficiency in the NIR band [36,37]. When incorporated into polymer matrices, it can convert absorbed NIR light into thermal energy, increasing the temperature of nanocomposites. The photothermal effect renders it an optimal candidate material for fabricating new type of photomechanical smart actuators. Furthermore, free standing GO films can be easily prepared by vacuum-assisted filtration macroscopic assembly of GO dispersions. As a result, GO can act as both photothermal heater and supporting matrix in the smart actuator.

Herein, we describe the fabrication of a novel NIR light-driven bilayer actuator, via a facile two-step vacuum filtration method. Our bilayer actuator consists a layer of GO, and a layer of GO/PNIPAM (GP) hybrid. The GO layer was formed via the by filtration method, and subsequently coated with a layer of GO/Poly(N-isopropylacrylamide) (GO/PNIPAM, GP) by vacuum-assisted filtration assembly. The thermo-responsive PNIPAM swells below the lower critical solution temperature (LCST,  $\sim 32$  °C) and shrinks above the LCST in water [38]. The NIR-absorbing GO sheets convert absorbed NIR light into thermal energy, which triggers the shrinkage of PANIPAM chains. Since the shape of the GO layer remains unaffected by the NIR light, repeated cycles of NIR light irradiations induce the asymmetric shrinkage/relaxation of the bilayer, thus endowing the reversible bending/unbending capability of the bilayer actuator.

Intriguingly, our bilayer actuator has shown “templated” bending orientations, and displays a shape memory effect, which can be attributed to the incomplete recovery of PNIPAM chains. Owing to this shape memory effect, complex performance such as twist has been achieved, and a smart NIR light-driven forklift truck has been constructed.

## 2. Experimental

**2.1 Materials.** Graphite was purchased from Uni-Chem. N, N-dimethyl formamide (DMF), Ether, ethanol, N-isopropylacrylamide (NIPAM), and 2,2'-Azobis-(isobutyronitrile) (AIBN) were purchased from Sinopharm Chemical Reagent Co., Ltd. NIPAM was recrystallized from a mixture of hexane and benzene (5:1 v/v). AIBN was recrystallized from ethanol.

**2.2 Synthesis of PNIPAM and GP mixture.** A typical procedure for synthesizing PNIPAM was performed as follows: the NIPAM (1g) was first dispersed in ethanol (10 mL) under the protection of N<sub>2</sub> flow, then the initiator AIBN (5.8 mg) was added and the polymerization was carried out at 70 °C for 2 hours. Afterwards, the products were precipitated in a large excess of ether, and the white polymer was collected by filtration, dried at 40 °C under vacuum overnight. The molecular weight of PNIPAM is 8049 Da (Fig. 1(a)).

PNIPAM (3 mg) and GO (25 mg) were mixed together in water (10 ml) for 24 hours at room temperature, denoted as GP (Fig. 1(b)).

**2. 3 Fabrication of soft GO/GP bilayer actuator.** To prepare the GO/GP bilayer film, GO aqueous (0.5 mL, 5 mg/mL) dispersion was filtrated through an acetate fiber Millipore filter (0.45  $\mu\text{m}$  in pore size and 47 mm in diameter). Subsequently, the GP (10 ml, 2.8 mg/mL) aqueous dispersion was filtrated through the first layer to form the bilayer actuator.

**2. 4 Characterization.** The thicknesses were carefully determined using scanning electron microscopy (SEM). SEM images were obtained with SEM (Quanta 400 FEG). SEC analysis was conducted on a modular system consisting of a Waters 1515 pump, a 717 plus autosampler, and a 2410 refractive index detector. DMF was used as the mobile phase at a flow rate of 1.0 mL/min at 40 °C. Thermogravimetric analysis (TGA) was carried out on a Perkin-Elmer Pyris 6 TGA instrument thermal analyzer at a heating rate of 10 °C /min under N<sub>2</sub> atmosphere. X-ray diffraction (XRD) analysis was performed on X'Pert-Pro MPD diffractometer with a Cu K $\alpha$  radiation source at room temperature (the angle measurement accuracy is 0.02°). The sample was heated on the hot stage at 45 °C. Atomic Force Microscope (AFM, Dimension Icon) images were obtained in the tapping mode on a Multimode 8 model scanning probe microscope, for which the GO dispersion was drop-casted onto freshly cleaved mica surfaces. Attenuated Total Reflectance Fourier Transform Infrared (ATR-FTIR) spectra were obtained with Bruker Vertex 70. Mechanical properties at room temperature were tested by Instron-3365 with gauge length of 10 mm, at the loading rate of 0.5 mm/min, and the relative humidity was 50% during the tensile test.

The bending/unbending process of GO/GP film and GO/GP strip were recorded with a digital camera (Canon EOS 70D). The bending curvature of the actuator was determined by fitting the optical image of the curved strip to a circle with a certain size (Fig. S5). A NIR light source (250 W, 0.76~25  $\mu\text{m}$ , Philips BR125) was used for photoactuation. The temperature change of the samples was recorded in real time by an infrared camera (E40, Flir system). The stress generated by the actuator strip was measured on the universal testing machine (KJ-1065A) with on/off the NIR light irradiations.

### **3. Results and Discussion**

#### **3.1 Preparation and characterization of GP and GO/GP**

As shown in Fig. 2, bilayer actuators were fabricated via a two-step vacuum filtration method. The GO layer was first prepared by vacuum filtration, and then the aqueous dispersion of GP was filtered through the GO layer to form the bilayer, as a result of the vacuum-assisted self-assembly. GO contains a variety of oxygen containing functional groups, such as epoxy groups, carboxylic acid groups and hydroxyl groups, which provide abundant active sites for forming hydrogen bonds [26], and hence the amide groups in PINPAM can lead the polymer to attach to the GO sheets via hydrogen bonds [39-41]. The AFM image (Fig. S1) of an individual GP sheet shows hairy surfaces, indicating the interaction between GO and PINPAM [41,42]. The mass fraction of PNIPAM in GP layer was determined through TGA curves (Fig. 3(a)) by measuring the weight loss between 350 °C and 500 °C. The

grafted polymer was 5.9 wt% which was less than feed ratio, corresponding to the volatilization of stored water in the polymers. All the samples show a certain weight loss below 100 °C, attributable to the volatilization of stored water in the film, which is essential for the swelling/deswelling transitions of PNIPAM chains [43]. Furthermore, we examined the FTIR spectrum to verify the chemical bonds between GO and GP film. (Fig. S2)

To further investigate the structure of GO/GP hybrids, XRD patterns of GO, GP, and GO/GP films were recorded (Fig. 3(b)). The peak for pure GO was observed at  $2\theta = 9.08^\circ$ , suggesting that the interlayer distance is 9.74 Å, agreeing well with previous literatures [44-47]. When the PNIPAM is intercalated between the GO sheets via hydrogen bond, the peak shift to  $7.85^\circ$ , revealing the increased interlayer distance of 11.24 Å. Meanwhile, the GO/GP films show a peak at  $7.64^\circ$  with almost the same position to that of GP films, and a broad peak centered at  $9.08^\circ$  of bilayer films, which verifies the bilayer structure.

Fig. 3(c) shows the temperature variation of the nanocomposite films upon photoirradiation of NIR. It increased from room temperature to 48 °C within 1.5 min of NIR light irradiation, and then decreased to room temperature within 4.5 min after the light was turned off, demonstrating the effective photothermal conversion of GO, which can cause the temperature switch between above- and below- LSCST of PNIPAM. In addition, GO can serve as supporting matrices in the bilayer actuator. Upon photoirradiation, the film temperature rapidly increases to the LCST of

PNIPAM. Volume contraction occurred along the whole film caused by the shrinkage of PNIPAM chains in GP layer, while the layer of GO exhibited fewer changes due to the lack of PNIPAM chains. Consequently, the films bent toward the GP films as shown in Fig. 3(d) and Supplementary Movie S1. Upon irradiation, the device bends along a central axis. The final shape and bending angle are determined by the size and shape of the substrate of the GP circular film, as well as the content of GP. It is noteworthy neither GP nor GO film alone bends significantly upon irradiation (Fig. S3 and Fig. S4), and the robust attachment of GP to GO enables the contraction of GP layer upon irradiation to be translated into device bending. When the light is switched off, the device subsequently opens (unbends), showing the reversible deformation in response to the on/off switch of light irradiation.

### 3.2 Investigation of the shape memory effect of the GO/GP bilayer actuator.

Interestingly, the GO/GP strips, which were cut from the original pre-bending circular GO/GP films, have shown a shape memory effect. The bimorph is cut into a strip (dimension of 20 mm  $\times$  5 mm) along varied orientations relative to the pre-bending axis (Fig. 4). Strip GO/GP-P is cut from the direction parallel with bending axis (Fig. 4(a)), strip GO/GP-V is cut from the direction perpendicular to the bending axis (Fig. 4(b) and Supplementary Movie S2), and strip GO/GP-45° is cut from the direction in 45 degree with the bending axis (Fig. 4(c)). One end of the strip was clamped. All the strips were heated by the NIR light for 2 min. Interestingly, the bending behaviors of the rectangular strip depend on the cutting orientation. The

parallel strip did not show any obvious bending upon the NIR light irradiation of 2 min. Under the same conditions, the vertical strip exhibited bending like the original films. Furthermore, strip GO/GP-45° noticeably twists under the NIR light. These results collectively reveal that the GO/GP actuator has shape memory effect. In other words, the bending deformation of the individual rectangular strips replicate their respective deformations exhibited before they were cut from the circular actuator.

More importantly, all the GO/GP devices bend in the same way over many bending/unbending cycles, indicating that the bending direction is permanently templated into the actuator. To rationalize this behavior, we defined the shape of the circular GO/GP film after bending upon NIR irradiation as the “permanent shape”. Because the circular film is symmetric, it tends to bend into a tube configuration, which minimizes the resistance to bending [27]. And then all parts of circular film can “memorize” this state. After the light is turned off, they have the ability to recover to the unbent state. Also, they are able to bend back to the tube shape when the light is switched on again (temperature increased). Therefore, each portion of the circular bilayer device is templated to bend in the orientation along which it originally bent as part of the uncropped “parent” circular actuator (Fig. 4), eventually enabling the reproducible shape change of the materials with temperature variations. This reproducible bending behavior is considered to be responsible for the shape memory effect observed in our bilayer actuator.

To further understand the mechanism of shape memory effect of our actuator, we investigated the structural and conformational changes of PNIPAM intercalated between GO nanosheets. It is acknowledged that PNIPAM chains undergo a structural reorganization from expanded random-coil to tightly packed globule above LCST in water [38]. Fan et al., have fabricated prepared the GO-PNIPAM hybrids via in situ free-radical polymerization [41], and found that the structural recognition of PNIPAM chain on substrate is the same as that in water, that is, when GP was heated above LCST of PNIPAM, the shrinkage and “coil-to-globule” transition of the PNIPAM chains occurs on GO surfaces.

Our study unveils that the PNIPAM intercalated between GO nanosheets exhibits the structure variation different from that in water or on 2D substrate. Specifically, the curvature-time curve of strip can be divided into three parts (Fig. 5(a)). The curvature was determined by fitting the curved strip using a circle with a certain size (Fig. S5). The Fig. 5(b) depicts the GO/GP strip model at the three regimes. In the first regime ( I ), the curvature has rapidly increased. When subject to NIR irradiation, GO adsorbs NIR light and photothermally increases the local temperature, and then the intercalated PNIPAM shows the “coil-to-globule” transition as demonstrated above. In the second regime ( II ), when the light is turned off, the bent GO/GP strip recovers to its original shape immediately. PNIPAM is subjected to the “globule-to-coil” transition, which is relying on the content of water in the GO-PNIPAM hybrids. Hence the intercalated water between GO nanosheets contributes to the rapid recovery of the strip. In the third

regime (III), the recovery speed decreases. This can be rationalized as follows: with the consumption of the intercalated water, the polymer only can absorb extra water from environment, which makes the water-dependent relaxation slower than that in the second regime, that is, the configurations of PNIPAM chains were partly locked. Due to the low content of surrounding water and confined effect of GO layers, PNIPAM chains can not transit to the original state completely, which is crucial for the shape memory effect. Accordingly, compared with the initial curvature, the strip has not completely recovered.

We heated the GO/GP film by hot plate to imitate the irradiation process and investigated the interlayer space of GO and GP. As the temperature increased from room temperature to 45 °C, the peak position of GO shifted from 9.08° to 10.68° (the change of interlayer space from 9.73 Å to 8.27 Å), indicating the loss of intercalated water molecules (Fig. 5(c)), and the peak position of GO/GP has shifted from 7.64° to 8.92° (Fig. 5(d)) (the interlayer space changes from 11.56 Å to 9.90 Å), suggesting the shrinkage of PNIPAM chains. These results have demonstrated the microstructure change of the bilayer actuator at the first stage. After cooling, the GO peak position returned to the 9.08°, which indicated the GO absorbed the water from the environment and recovered the interlayer lamellar structure. However, the GO/GP peak position changed to 7.82°, slightly different from the initial peak position of GO/GP (7.64°), suggesting PNIPAM chains have not completely swollen between the GO sheets. As a

result, the strip has not completely recovered to the initial state, which is consistent with the curvature changes in the Fig. 5(a).

We further assessed the reproducibility of actuator, which is an important property for the practical applications. Fig. 6(a) displays five cycles of bending/unbending performance of the rectangular strip cut perpendicular to the initial bending axis. When exposed to cycling NIR light, the films show bending/unbending changes, which synchronized with the on/off switch of the light irradiations and were highly reversible without noticeable deterioration, demonstrating the device's instant and reversible response to the NIR light.

#### 4. Smart device

The stress generated by the actuator under NIR irradiation was further examined by subjecting a strip-shaped sample (3×30 mm) to a constant strain (0.5 %) using universal material testing machine. The stress generated by the actuator of GO/GP-V was 10 MPa (Fig. 6(b)) but the ultimate tensile strength of GO/GP-P (Fig. 6(c)) was only 3 MPa (Fig. 6(d)) like pure GO (Fig. 6(c)). The stress is nearly two orders of magnitude higher than that of mammalian skeletal muscle (0.35 MPa) [48]. These results suggest that only rectangular bilayers cut from a certain orientation contributes to the enhancement of the stress generated by the actuator, corroborating the presence of the shape memory effect of the actuator. Also, the tensile test results show that the GO/GP films have beneficial machine properties with higher modulus (8.42 GPa) (Fig S6)

Motivated by the unique anisotropic structure and excellent bending performance of GO/GP bilayer papers, we further designed and fabricated an interesting smart “forklift truck”. As mentioned above, the GO/GP paper bend up and generated higher stress under the NIR light than one layer of GO or GP. By immobilizing one edge of the GO/GP paper, the “forklift truck” can lift up the foam substrate spontaneously and continuously under the NIR light. In this process, the cube foam acts as a heavy object which has been fixed on the GO/GP. With the NIR light turned on, the forklift truck would lift the foam, which was shown in the Fig. 7(a~c) and Fig. 7(d~f), corresponding to the first regime ( I ). And with the light off, although the moisture would increase, the foam was still lifted due to the “lock” effect in the Fig. 7(g) corresponding to the second regime ( II ). After a while, the Fig. 7(h) displays the final state of the “forklift truck”, corresponding to the third regime (III). The dynamic bending and the lifting forklift show that the GO/GP bilayer paper has great potential in biomimetic applications.

#### **4. Conclusions**

In this work, a facile strategy has been developed to fabricate a NIR light-driven GO/GP bilayer actuator. The unique characteristics of GO/GP bilayer film enable it to form high performance NIR light-driven actuator, showing an outstanding bending/unbending behaviour. The actuator shows interesting shape memory behaviour with the bending orientation permanently templated into the actuator from the first application of NIR light. Inspiringly, this study offers a strategy for producing

GO/GP bilayer actuators for complex deformation such as twist, and also provides a broad platform for the development of smart device. Furthermore, the generated force and stress test demonstrate that the GO/GP paper has great potential in the biomimetic muscle. As a specific application, the “forklift truck” is designed to show promising practical applications of the GO/GP actuator. We envisage that this composites paper enjoy potentials to promote the future development of many fields, such as artificial muscles, robotics, smart household materials and sensing.

#### AUTHOR INFORMATION

##### **Corresponding Author**

\* E-mail: yangxiaoming@suda.edu.cn.

##### **Notes**

The authors declare no competing financial interest.

#### ACKNOWLEDGMENT

**Ze Chen** is currently a M.S. candidate in the Department of Chemistry of Soochow University. His research is focused on actuators and supercapacitors.

**Rui Cao** obtained his M.S. degree in the Department of Chemistry of Soochow University (2017). His research is focused on actuators.

**Yuanhang Ge** is currently a M.S. candidate in the Department of Chemistry of Soochow University. His research is focused on actuators and supercapacitors.

**Sunjie Ye** received her Ph.D. from School of Chemistry and Chemical Engineering, Nanjing University in 2011 (Ph.D. Supervisor: Professor Yun Lu). She was a Wellcome Trust ISSF Junior Development Investigator (2012-2014) in University of Leeds, and subsequently a postdoctoral research fellow in School of Physics and Astronomy (2014-present), University of Leeds. Her research focuses on the design and construction of novel nanomaterials (e.g., gold nanostructures, polymer/metal or semiconductor nanocomposites), investigating their structural

and optical properties (e.g. Surface enhanced Raman Scattering, Surface Plasmon Resonance), and exploring their property-based applications, such as biosensing, bioimaging, phototherapy and catalysis.

**Yingfeng Tu** received his B.S. (1998) and Ph. D. degree (2003) in Polymer Chemistry and Physics from Peking University. During that period, he studied in the Department of Chemistry at The Chinese University of Hong Kong as a joint research student for two years (1999-2000, 2001-2002). He worked as a postdoctoral researcher at The University of Akron (2004-2009), and then joined Soochow University in 2009 as a full professor. His current research interests include: 1) novel polymerization techniques for functional materials; 2) supramolecular liquid crystals.

**Xiaoming Yang** received her B.S. degree (2000) and M.S. degree (2003) in Polymer Science and Engineering from Sichuan University and Ph. D. degree (2006) in Polymer Physics and Chemistry from Nanjing University. She joined Soochow University at 2006. She worked as a postdoctoral researcher in Hong Kong Polytechnic University (2008-2010) and a visiting scholar in University of Pennsylvania (2015-2016). Now, she is an associated professor of Soochow University. Her research focuses on: 1. graphene/polymer nanocomposites. 2. Liquid crystalline polymer. 3. Nanostructure of conducting polymer.

The financial support from China Postdoctoral Science Foundation (2013M541715, 2014T70541), a Project Funded by the Priority Academic Program Development of Jiangsu Higher Education Institutions (PAPA) are gratefully acknowledged.

## REFERENCES

- (1) S. Kawata, H. B. Sun, T. Tanaka, K. Takada, Finer features for functional microdevices, *Nature* 412(2001) 697–698.
- (2) M. Y. Ji, N. Jiang, J. Chang, J. Q. Sun, Near-Infrared Light-Driven, Highly Efficient Bilayer Actuators Based on Polydopamine-Modified Reduced Graphene Oxide, *Adv. Funct. Mater.* 24(2014) 5412–5419.
- (3) K. Malachowski, M. Jamal, Q. R. Jin, B. Polat, C. J. Morris, D. H. Gracias, Self-folding single cell grippers, *Nano Lett.* 14(2014) 4164–4170.

- (4) Y. L. Sun, W. F. Dong, R. Z. Yang, X. L. Meng, Q. D. Zhang, H. Chen, B. Sun, Dynamically tunable protein microlenses. *Angew. Chem. Int. Ed.* 51(2012) 1558–1562.
- (5) H. H. Cheng, Y. Hu, F. Zhao, Z. L. Dong, Y. H. Wang, N. Chen, Z. P. Zhang, L. T. Qu, Moisture-Activated Torsional Graphene-Fiber Motor, *Adv. Mater.* 26(2014) 2909–2913.
- (6) H. Xia, J. A. Wang, Y. Tian, Q. D. Chen, X. B. Du, Y. L. Zhang, Y. He, H. B. Sun, Ferrofluids for Fabrication of Remotely Controllable Micro-Nanomachines by Two-Photon Polymerization, *Adv. Mater.* 22(2010) 3204–3207.
- (7) G. Rydzek, T. G. Terentyeva, A. Pakdel, D. Golberg, J. P. Hill, K. Ariga, Simultaneous Electropolymerization and Electro-Click Functionalization for Highly Versatile Surface Platforms, *ACS Nano.* 8(2014) 5240–5248.
- (8) M. Jamal, A. M. Zarafshar, D. H. Gracias, Differentially photo-crosslinked polymers enable self-assembling microfluidics, *Nat. Commun.* 2(2011) 527.
- (9) P. Brochu, Q. Pei, Advances in Dielectric Elastomers for Actuators and Artificial Muscles, *Macromol. Rapid Commun.* 31(2010) 10–36.
- (10) C. G. Hu, L. Song, Z. P. Zhang, N. Chen, Z. H. Feng, L. Qu, T. Tailored, Graphene Systems for Unconventional Applications in Energy Conversion and Storage Devices, *Energy Environ. Sci.* 8(2015) 31–34.

- (11) J. Kim, J. K. Koh, B. Kim, J. H. Kim, E. Kim, Nanopatterning of Mesoporous Inorganic Oxide Films for Efficient Light Harvesting of Dye-Sensitized Solar Cells, *Angew. Chem. Int. Ed.* 51(2012) 6864–6869.
- (12) A. Villanueva, C. Smith, S. Priya, A Biomimetic Robotic Jellyfish (Robojelly) Actuated by Shape memory Alloy Composite Actuators, *Bioinspiration Biomimetics*. 6(2011) 036004.
- (13) D. L. Thomsen, P. Keller, J. Naciri, R. Pink, H. Jeon, D. Shenoy, B. R. Ratna, Liquid crystal elastomers with mechanical properties of a muscle, *Macromolecules* 34(2001) 5868–5875.
- (14) D. D. Han, Y. L. Zhang, H. B. Jiang, H. Xia,; J. Feng, Q. D. Chen, H. L. Xu, H. B. Sun, Moisture-responsive graphene paper prepared by self-controlled photoreduction, *Adv. Mater.* 27(2015) 332–338.
- (15) J. Mu, C. Hou, H. Wang, Y. Li, Q. Zhang, M. Zhu, Origami-Inspired Active Graphene-Based Paper for Programmable Instant Self-Folding Walking Devices, *Sci. Adv.* 1(2015) e1500533.
- (16) C. Ohm, M. Brehmer, R. Zentel, Liquid Crystalline Elastomers as Actuators and Sensors, *Adv. Mater.* 22(2010) 3366–3387.
- (17) Z. Hu, X. Zhang, Y. Li, Synthesis and application of modulated polymer gels, *Science* 269(1995) 525–527.

- (18) E. Smela, Conjugated polymer actuators for biomedical applications, *Adv. Mater.* 15(2003) 481–494.
- (19) W. Nakanishi, K. Minami, L. K. Shrestha, Q. M. Ji,; J. P. Hill, K. Ariga, Bioactive nanocarbon assemblies: Nanoarchitectonics and applications, *Nano Today* 9(2014) 378–394.
- (20) H. B. Jiang, Y. L. Zhang, D. D. Han, H. Xia,; J. Feng, Q. D. Chen, Z. R. Hong, H. B. Sun, Bioinspired Fabrication of Superhydrophobic Graphene Films by Two-Beam Laser Interference, *Adv. Funct. Mater.* 24(2014) 4595–4602.
- (21) J. Zhang, L. Song, Z. P. Zhang, N. Chen, L. T. Qu, Environmentally responsive graphene systems, *Small* 10(2014) 2151–2164.
- (22) W. Xiong, Y. S. Zhou, W. J. Hou, L. J. Jiang, Y. Gao, L. S. Fan, L. Jiang, J. F. Silvain, Y. F. Lu, Bulk metallic glass composite with good tensile ductility, high strength and large elastic strain limit, *Sci. Rep.* 4(2014) 5302.
- (23) W. Guo, C. Cheng, Y. Wu, Y. Jiang, J. Gao, D. Li, L. Jiang, Bio-inspired two-dimensional nanofluidic generators based on a layered graphene hydrogel membrane, *Adv. Mater.* 25(2013) 6064–6068.
- (24) H. Cheng, J. Liu,; Y. Zhao, C. Hu, Z. Zhang, N. Chen, L. Jiang, L. Qu, Graphene Fibers with Predetermined Deformation as Moisture-Triggered Actuators and Robots, *Angew. Chem., Int. Ed.* 52(2013) 10482–10486.

- (25) D. D. Han, Y. L. Zhang, Y. Liu, Y. Q. Liu, H. B. Jiang, B. Han, X. Y. Fu, H. Ding, H. L. Xu, H. B. Sun, Bioinspired Graphene Actuators Prepared by Unilateral UV Irradiation of Graphene Oxide Papers, *Adv. Funct. Mater.* 25 (2015) 4548–4557.
- (26) A. Buchsteiner, A. Lerf, J. Pieper, Water dynamics in graphite oxide investigated with neutron scattering, *J. Phys. Chem. B* 110(2006) 22328–22338.
- (27) S. Park; J. An, J. W. Suk, R. S. Ruoff, Graphene-Based Actuators, *Small* 6(2010) 210–212.
- (28) D. D. Han, Y. L. Zhang, Y. Liu, Y. Q. Liu, H. B. Jiang, B. Han, X. Y. Fu, H. Ding, H. L. Xu, H. B. Sun, Bioinspired Graphene Actuators Prepared by Unilateral UV Irradiation of Graphene Oxide Papers, *Adv. Funct. Mater.* 25(2015) 4548–4557.
- (29) Niu, D.; Jiang, W. T.; Liu, H. Z.; Zhao, T. T.; Lei, B.; Li, Y. H.; Yin, L.; Shi, Y. S.; Chen, B. D.; Lu, B. H. Reversible Bending Behaviors of Photomechanical Soft Actuators Based on Graphene Nanocomposites, *Sci.Rep.* 6(2016) 27366.
- (30) M. F. Tsai, S. H. G. Chang, F. Y. Cheng, V. Shanmugam, Y. S. Cheng, C. H. Su, C. S. Yeh, Au Nanorod Design as Light-Absorber in the First and Second Biological Near-Infrared Windows for in Vivo Photothermal Therapy, *ACS Nano* 7(2013) 5330–5342.
- (31) C. Raimondo, N. Crivillers, F. Reinders, F. Sander, M. Mayor, P. Samorì, Optically switchable organic field-effect transistors based on photoresponsive gold

nanoparticles blended with poly(3-hexylthiophene), *Proc. Natl. Acad. Sci. U.S.A.*

109(2012) 12375–12380.

(32) N. M. Idris, M. K. Gnanasammandhan, J. Zhang, P. C. Ho, R. Mahendran, Y.

Zhang, In vivo photodynamic therapy using up conversion nanoparticles as remote-

controlled nanotransducers, *Nat. Med.* 18(2012) 1580–1585.

(33) X. Zhang, Z. B. Yu, C. Wang, D. Zarrouk, J. W. T. Seo, J. C. Cheng, A. D.

Buchan, K. Takei, Y. Zhao, J. W. Ager, J. J. Zhang, M. Hettick, M. C. Hersam, A. P.

Pisano, R. S. Fearing, A. Javey, Photoactuators and motors based on carbon nanotubes

with selective chirality distributions, *Nat. Commun.* 5(2014) 2983.

(34) E. Wang, M. S. Desai, S. W. Lee, Light-Controlled Graphene–Elastin Composite

Hydrogel Actuators, *Nano Lett.* 13(2013) 2826–2830.

(35) Y. Zhao, L. Song, Z. Zhang, L. Qu, Stimulus-responsive graphene systems

towards actuator applications, *Energy. Environ. Sci.* 6(2013) 3520–3536.

(36) J. T. Robinson, S. M. Tabakman, Y. Liang, H. Wang, Z. Sanche, H. Casalongue,

D. Vinh, H. Dai, Ultrasmall reduced graphene oxide with high near-infrared

absorbance for photothermal therapy, *J. Am. Chem. Soc.* 133(2011) 6825–6831.

(37) M. Acik, G. Lee, C. Mattevi, M. Chhowalla, K. Cho, Y. Chabal, Unusual infrared-

absorption mechanism in thermally reduced graphene oxide, *Nat. Mater.* 9(2010) 840–

845.

- (38) C. Wu, X. H. Wang, Globule-to-coil transition of a single homopolymer chain in solution, *Phys. Rev. Lett.* 80(1998) 4092–4094.
- (39) Y. Q. Sun, C. Li, Y. X. Xu, H. Bai, Z. Y. Yao, G. Q. Shi, Chemically converted graphene as substrate for immobilizing and enhancing the activity of a polymeric catalyst, *Chem. Commun.* 46(2010) 4740–4742.
- (40) M. Fang, K. Wang, H. Lu, Y. Yang, S. Nutt, Covalent polymer functionalization of graphene nanosheets and mechanical properties of composites, *J. Mater. Chem.* 19(2009) 7098–7105.
- (41) J. Qi, W. Lv, G. Zhang, F. Zhang, X. Fan, Poly (N-isopropylacrylamide) on two-dimensional graphene oxide surfaces, *Polym. Chem.* 3(2012) 621–624.
- (42) L. Y. Kan, Z. Xu, C. Gao, General Avenue to Individually Dispersed Graphene Oxide-Based Two-Dimensional Molecular Brushes by Free Radical Polymerization, *Macromolecules* 44(2011) 444–452.
- (43) A. H. Liu, I. Honma, M. Ichihara, H. S. Zhou, Poly (acrylic acid)-wrapped multi-walled carbon nanotubes composite solubilization in water: definitive spectroscopic properties, *Nanotechnology* 17(2006) 2845–2849.
- (44) L. Ma, X. Yang, L. Gao, M. Lu, C. Guo, Y. Li, Y. Tu, X. Zhu, Synthesis and characterization of polymer grafted graphene oxide sheets using a Ce (IV)/HNO<sub>3</sub> redox system in an aqueous solution, *Carbon* 53(2013) 269–276.

(45) Y. Wu, R. Cao, L. Ji, W. Huang, X. Yang, Y. Tu, Synergistic toughening of bioinspired artificial nacre by polystyrene grafted graphene oxide, RSC Adv. 5(2015) 28085-28091.

(46) Y. H. Wu, R. Cao, G. X. Wu, W. H. Huang, Z. Chen, X. M. Yang, From ultratough artificial nacre to elastomer: Poly (n-butyl acrylate) grafted graphene oxide nanocomposites, Composites: Part A 88(2016) 156–64.

(47) R. Cao, Z. Chen, Y. H. Wu, Y. F. Tu, G. X. Wu, X. M. Yang, Precisely controlled growth of poly (ethyl acrylate) chains on graphene oxide and the formation of layered structure with improved mechanical properties, Composites: Part A 93(2017) 100–106.

(48) M. Ma, L. Guo, D. G. Anderson, R. Langer, Bio-inspired polymer composite actuator and generator driven by water gradients, Science 339(2003) 186–189.

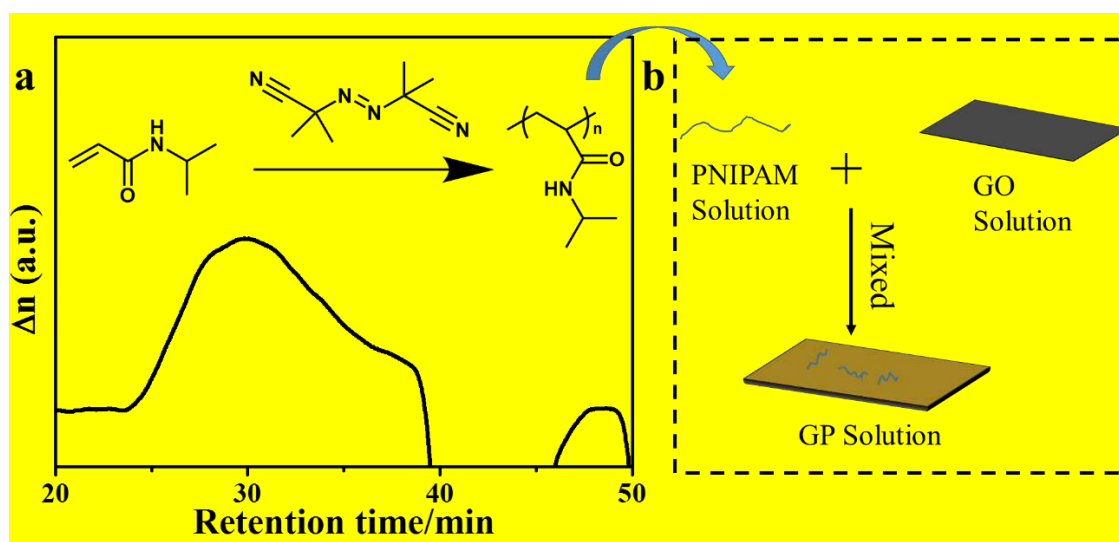


**Fig. 1.** (a) Synthesis of the PNIPAM by the free radical polymerization and the Size Exclusion Chromatography (SEC) curve of the obtained PNIPAM. (b) Schematic depiction of the synthesis of GP mixture.

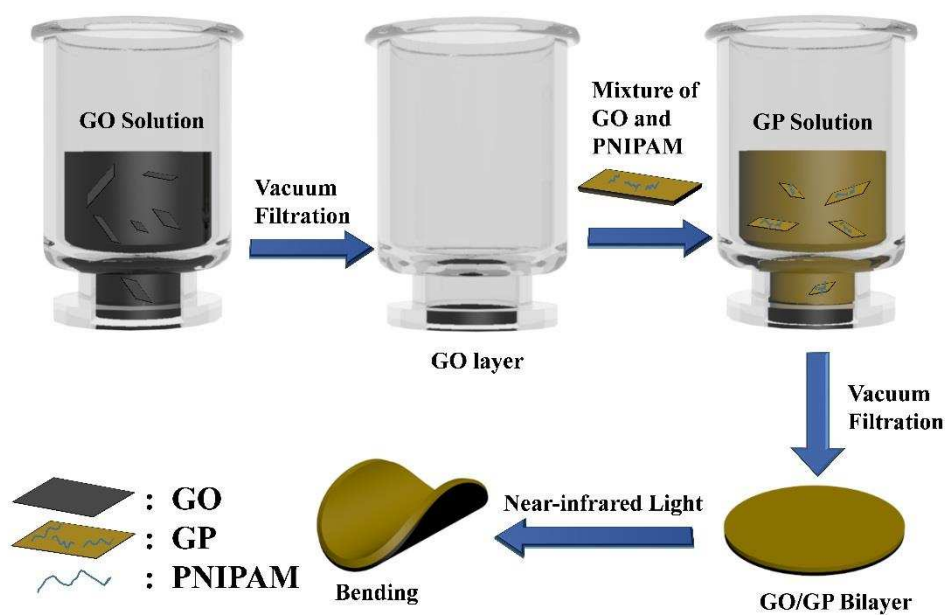


**Fig. 2.** Schematic illustration showing the preparation protocol of a GO/GP bilayer actuator, and the bending motion of the bilayer actuator, upon NIR light irradiation.

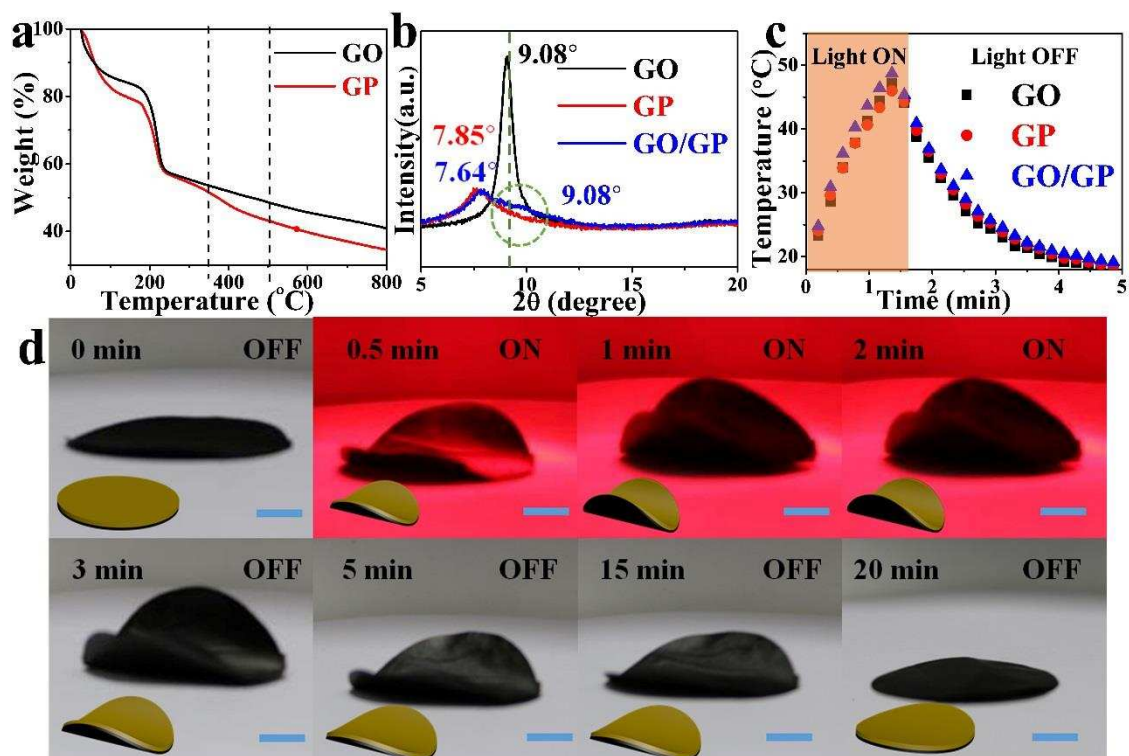


**Fig. 3.** (a) TGA curves of GO and GP film. (b) XRD curves of GO, GP, and GO/GP bilayer films. (c) Temperature measurement of GO, GP and GO/GP bilayer when light is turned on (Time, 1.5 min) and off (Time, 3.5 min) exposed to the NIR. (d) A series of optical images demonstrating the light-actuation process of bilayer of GO/GP films. (Scale bar: 1cm).

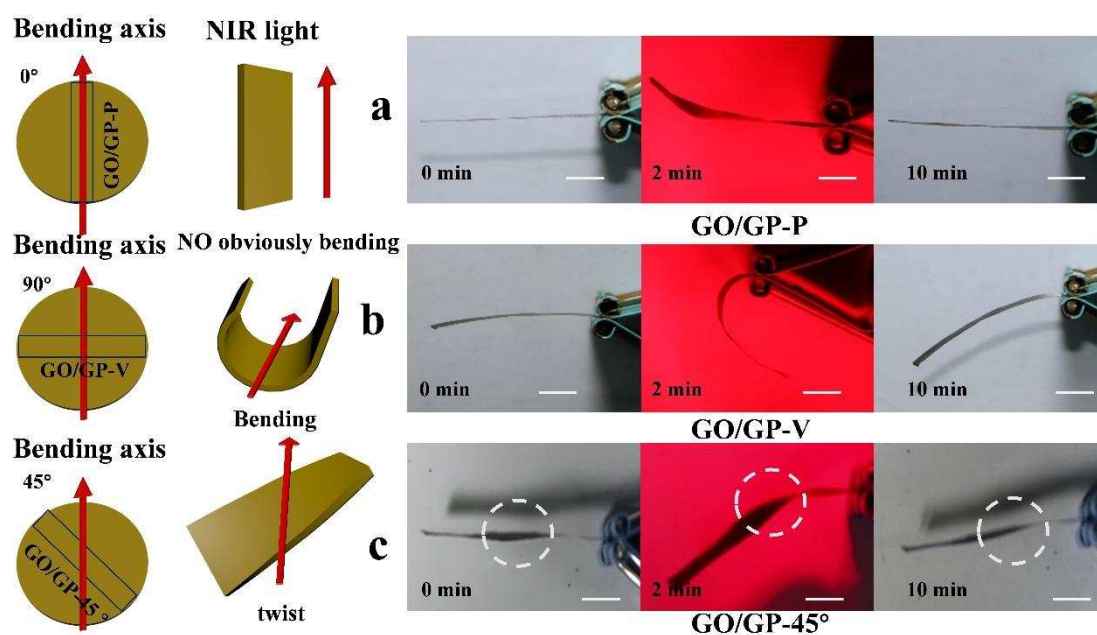


**Fig. 4.** (a, b) Rectangular strips cut from the same bilayer along different directions. (a) Along the direction parallel to the bending axis named as GO/GP-P. (b) Along the direction perpendicular to bending axis named as GO/GP-V. (c) Along the direction in 45 degree with the bending axis, named as GO/GP-45°. The arrows indicate the bending axis. (Scale bar: 1cm)

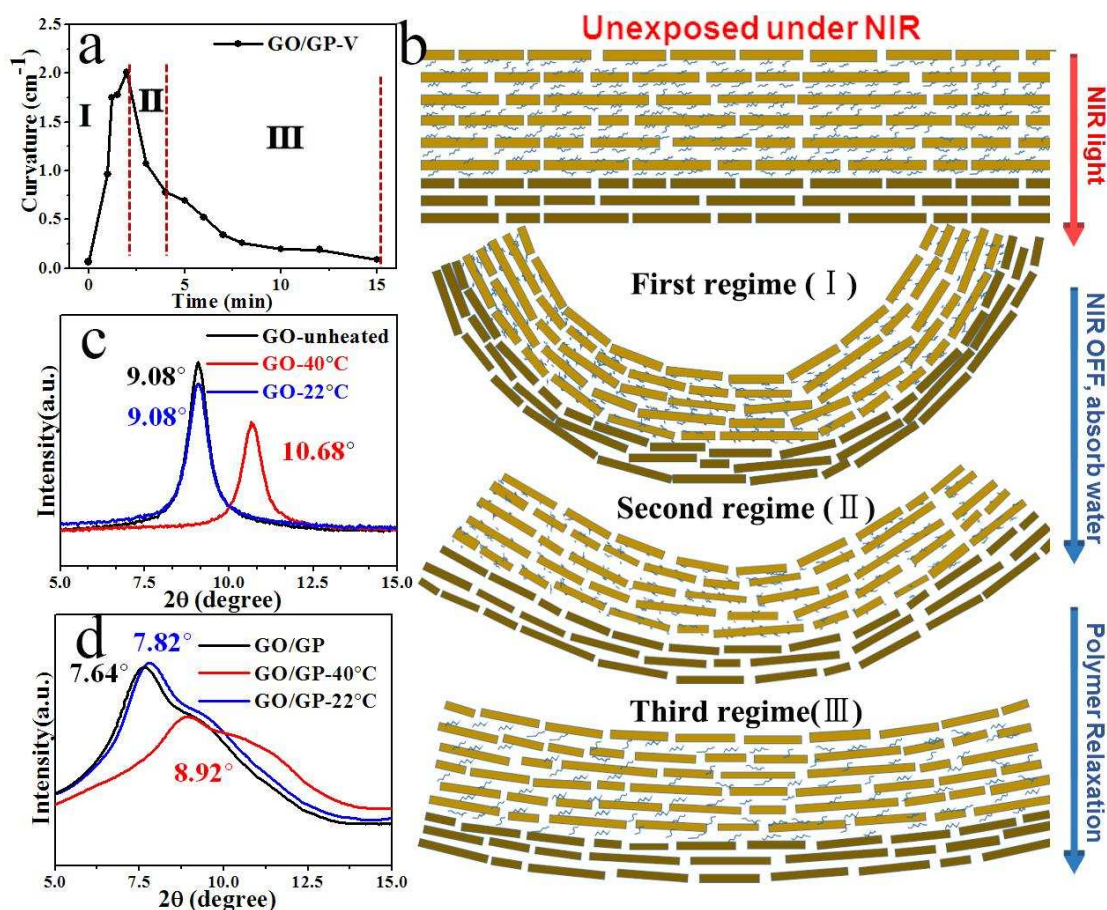


**Fig. 5.** (a) The plot of curvature versus time for the GO/GP-V during and after the of NIR light irradiation showing three distinct regimes; (b) Schematic illustration of the mechanical locomotion mechanism of the GO/GP thin film actuator. With the light turned on, the PNIPAM and water molecules intercalated between GO nanosheets make synergistic contributions to the bending/unbending deformation of GO/GP bilayer; XRD curves of the GO (c) and GO/GP (d) at the different temperatures.

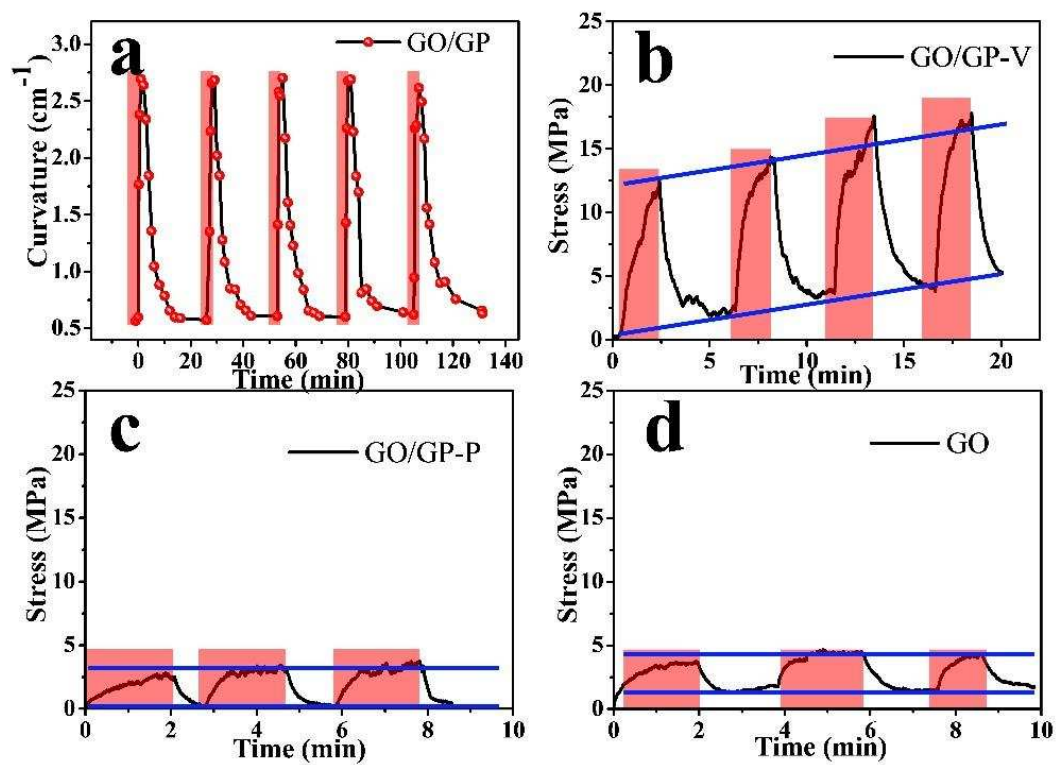


**Fig. 6.** (a) Reversible bending/unbending behaviors of the GO/GP bilayer actuator in response to repeated cycles of NIR light irradiations; Time-dependent stress generated by strips of (b) GO/GP-V, (c) GO/GP-P, (d) GO upon NIR light irradiation (red areas).

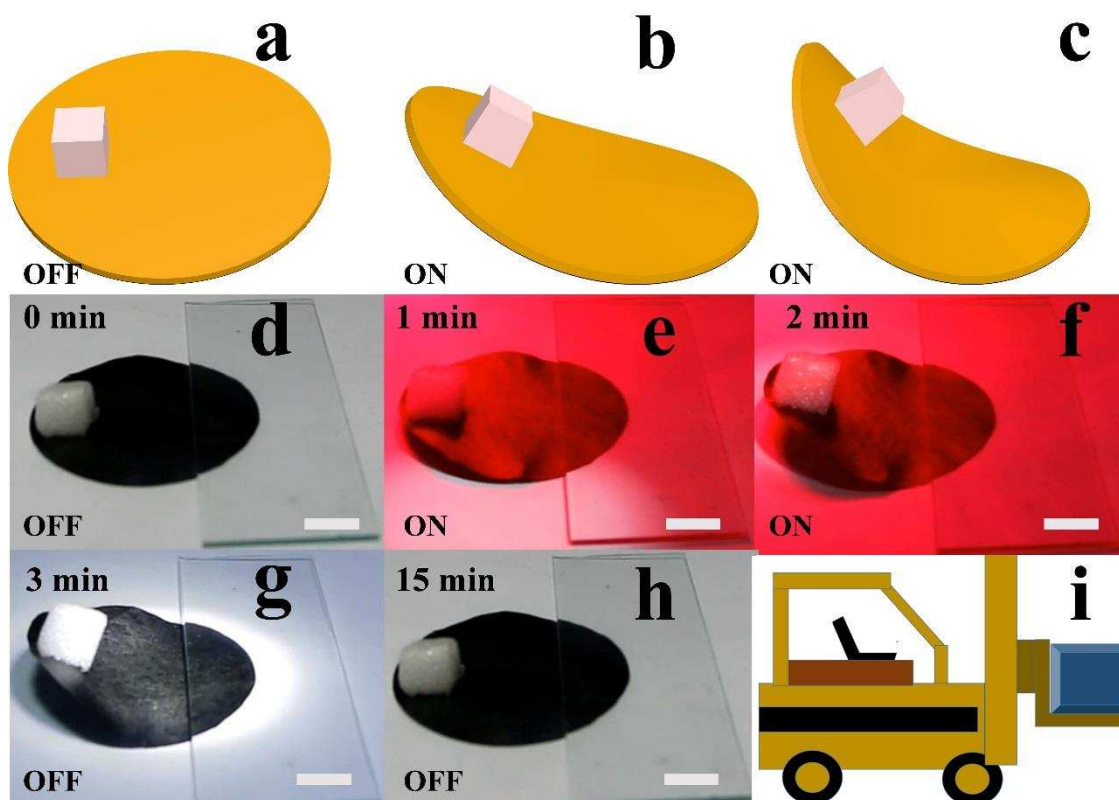


**Fig. 7.** (a-c) Schematic illustration of the lifting actuation of the “forklift truck” under NIR irradiation; (d-h) a series of optical images showing the smart “forklift truck” lifted the cube foam with the on/off switch of the NIR light (Scale bar: 1cm); (i) Cartoon illustration of the “forklift truck”.